

Excitation of the ground state rotational band in ^{20}Ne by 0.8 GeV protons

G. S. Blanpied, G. A. Balchin, G. E. Langston, and B. G. Ritchie*
University of South Carolina, Columbia, South Carolina 29208

M. L. Barlett, G. W. Hoffmann, and J. A. McGill†
University of Texas, Austin, Texas 78712

M. A. Franey and M. Gazzaly
University of Minnesota, Minneapolis, Minnesota 55455

B. H. Wildenthal

Drexel University, Philadelphia, Pennsylvania 19104

(Received 5 August 1983; revised manuscript received 13 April 1984)

Angular distributions for the scattering of 0.8 GeV polarized protons from the ground state rotational band in ^{20}Ne are reported. Cross sections and analyzing powers for protons exciting these states were measured with a high resolution spectrometer. Coupled channels and distorted wave Born approximation analyses of scattering data for the 0^+ , 2^+ , 4^+ , and experimentally unresolved 6^+ states are presented. The observed cross section data for the 0^+ , 2^+ , and 4^+ states are reproduced quite well with the coupled channels calculations, and the large hexadecapole deformation reported previously is confirmed. The distorted wave Born approximation results are equally good for the 0^+ angular distribution, but are a significantly poorer representation of the cross section data for the 2^+ and 4^+ states. Both calculations do equally well in explaining the 0^+ analyzing power data and both fail to explain the 4^+ analyzing power data past the region of the first maximum. The coupled channels results do a better job in explaining the 2^+ analyzing power data. The multipole moments of the deformed optical potential used in the coupled channels calculations are related to those of the matter distributions by Satchler's theorem. These are compared to the moments found using other hadronic probes, those of the charge distribution determined by electromagnetic measurements, and to moments from shell model and Hartree-Fock calculations.

I. INTRODUCTION

Coupled channels analyses of ~ 1 GeV proton inelastic scattering from light s - d shell nuclei and heavy rare earth nuclei have been shown to be generally successful, provided deformation and multistep processes are properly treated.¹⁻⁶ These collective rotational model calculations provide excellent descriptions of the data for the lowest 0^+ , 2^+ , and 4^+ states in $^{24,26}\text{Mg}$.⁶

The multipole moments of the empirically determined optical potentials, which are related to those of the deformed matter densities by Satchler's theorem,⁷ can be compared to the multipole moments of the charge densities obtained via electromagnetic measurements. Generally, the deduced $M(E2, \text{matter})$ moments are slightly smaller than those of the charge densities for ^{12}C , ^{24}Mg , and ^{26}Mg .^{2,6}

In these calculations the deformation of the radius of the optical potential is given by

$$R(\theta) = R_0(1 + \beta_2 Y_{20} + \beta_4 Y_{40} + \dots). \quad (1)$$

The results for ^{12}C and ^{24}Mg indicate that $\beta_4 \sim 0$, so that the hexadecapole moment is small, while β_4 for ^{26}Mg is somewhat larger. Low energy hadron scattering yields a β_4 for ^{20}Ne that is large ($\beta_4/\beta_2 \sim 0.5$).⁸⁻¹⁵ To improve the knowledge of deformations in s - d shell nuclei and fur-

ther study intermediate energy proton inelastic scattering from light, deformed nuclei, new data for $^{20}\text{Ne}(\vec{p}, p')$ at 0.8 GeV are presented here.

II. EXPERIMENT

The data were obtained using the High Resolution Spectrometer (HRS) of the Los Alamos Clinton P. Anderson Meson Physics Facility (LAMPF). The experiment consisted of scattering 0.8 GeV polarized protons from a ^{20}Ne gas target, enriched to 99.95%. Measured angular distributions and analyzing powers, A_y , extend from 5.3° to 26.3° c.m. for all states up to ~ 12 MeV. The (\vec{p}, p') data presented here are for the excitation of the (ground state, 0^+), (1.63 MeV, 2^+), (4.25 MeV, 4^+), and (8.7 MeV, $1^- + 6^+$) states in ^{20}Ne .

Since this was the first experiment at the HRS to use a gas target, some details are given here. Data were acquired for a ^{14}N gas target identical in geometry to the ^{20}Ne target, and for a ^{208}Pb foil. The ratios of the ^{14}N gas target data to previous ^{14}N measurements, which used a solid melamine target,¹⁶ determined the beam interaction volume in the gas target as a function of scattering angle. The interaction volume was found to be constant out to 6.8_{lab} , thereafter falling as $\sin^{-1}(\theta_{\text{lab}})$. The results are given in Fig. 1. The ratios of ^{14}N data for the well-

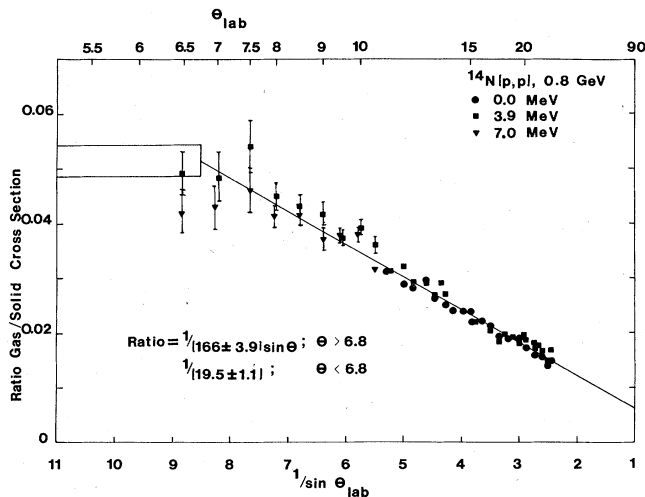


FIG. 1. The ratios of cross sections taken with a ^{14}N gas target to previous measurements (Ref. 16) employing a solid melamine target are given as a function of $\sin^{-1}(\theta_{\text{lab}})$. The laboratory scattering angle is also given at the top scale.

resolved 0.0, 3.9, and 7.0 MeV states are plotted versus the inverse of $\sin(\theta_{\text{lab}})$. The laboratory scattering angle is also given at the top scale of the figure for reference. Notice that the ratio changes by a factor of 3 over the measured region. Background from the Mylar windows of the targets interferes with the ^{14}N elastic peak inside 10°_{lab} , so only the ratios for the two excited states are used in this region. The ratio at 0° is calculated using the ^{208}Pb data normalized to those of Ref. 17, the gas pressure (3.16 atmospheres in Los Alamos where atmospheric pressure is 0.78 that at sea level), and the target thickness (including the bulge in the windows, 12.4 ± 0.1 cm). This ratio is computed to be 0.0513 ± 0.0030 . A chi-squared fit to the data using

$$\text{ratio} = 1/(a \sin \theta + b)$$

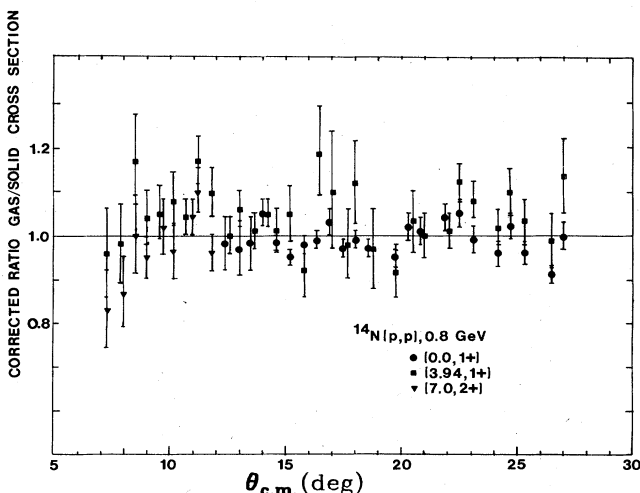


FIG. 2. The corrected ratio of gas/solid cross sections for the three ^{14}N states are given as a function of $\theta_{\text{c.m.}}$.

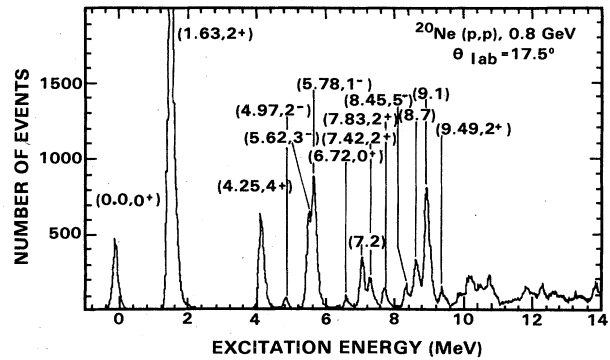


FIG. 3. A spectrum for $^{20}\text{Ne}(p,p)$ at 0.8 GeV and $\theta_{\text{lab}} = 17.5^\circ$ is presented. This angle is approximately the center of the angular range covered in this experiment.

results in $a = 166 \pm 3.9$ and $b = 0. \pm 0.0005$. This fit, shown in Fig. 1, was used to compute the absolute normalization of the present ^{20}Ne data with an overall uncertainty of about $\pm 10\%$. The corrected ratio of gas/solid cross sections for the three ^{14}N states are shown as a function of $\theta_{\text{c.m.}}$ in Fig. 2. This figure supports the result of the least-squares analysis that the overall uncertainty is $\leq \pm 10\%$. This correction factor is multiplied by 2 to account for the diatomic nature of ^{14}N vs monatomic molecules, when applied to ^{20}Ne . The ^{20}Ne and ^{14}N targets were filled to the same relative pressure in identical gas cells, so that the uncertainties due to target thickness and absolute pressure cancel. Both neon and nitrogen are close to ideal gases. The value of ρ/A for the gases, computed from the van der Waals equation, are 0.1304 for ^{20}Ne and 0.1308 for ^{14}N , while the ideal gas value is 0.1305.

The absolute scattering angle was determined to $\pm 0.05^\circ$

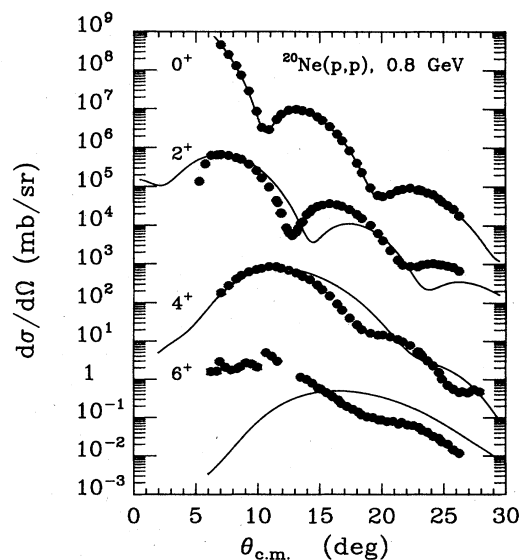


FIG. 4. Angular distributions of $^{20}\text{Ne}(p,p)$ at 0.8 GeV, for the 0^+ , 2^+ , 4^+ , and unresolved doublet (1^- , 6^+) are shown. The curves result from the DWBA calculations discussed in the text.

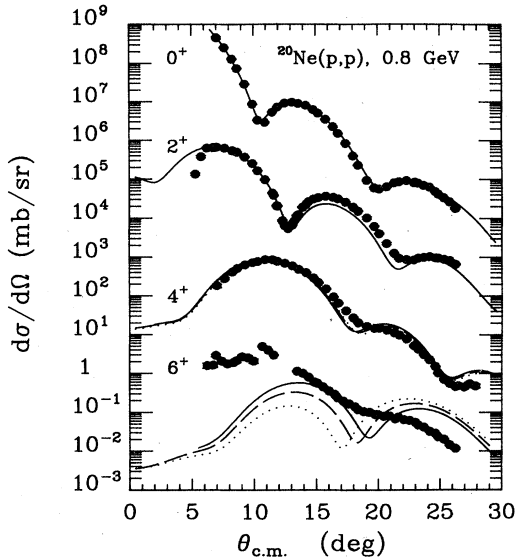


FIG. 5. Same as Fig. 4 with the curves resulting from the coupled channels calculations discussed in the text. The solid lines result from $\beta_6 = +0.03$, the dashed lines from $\beta_6 = 0$, and the dotted lines from $\beta_6 = -0.03$.

by comparing the ^{208}Pb data taken here to those of Ref. 17. The energy resolution ($\Delta E \sim 140$ keV) allowed the extraction of many peak areas from the spectra. One spectrum for $^{20}\text{Ne}(p,p)$ which is approximately centered in the angular range covered is given in Fig. 3. A tentative identification is made of observed peaks up to 9.49 MeV. The

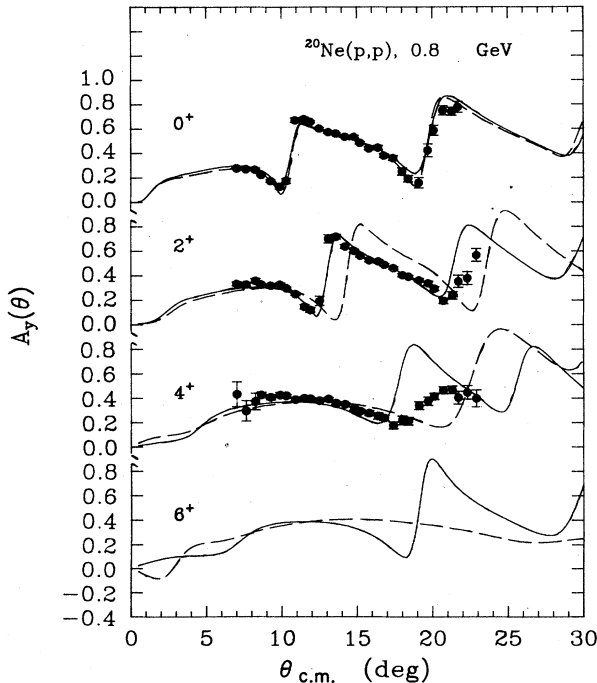


FIG. 6. Analyzing powers for $^{20}\text{Ne}(\bar{p}, p')$ at 0.8 GeV, for the 0^+ , 2^+ , and 4^+ states are shown. The data for the unresolved 6^+ are not shown. The curves result from the coupled channels (solid) and DWBA (dashed) calculations discussed in the text.

resulting angular distributions for the 0^+ , 2^+ , 4^+ , and unresolved 6^+ states are presented twice in Figs. 4 and 5, while the analyzing power [$A_y(\theta)$] data are presented in Fig. 6.

III. ANALYSIS

Distorted wave Born approximation (DWBA) calculations using a spherically symmetric optical potential are shown as solid lines in Fig. 4 and as dashed lines in Fig. 6. Coupled channels calculations using a deformed optical potential have been made using the code ECIS (Ref. 18), in which the 0^+ , 2^+ , 4^+ , and 6^+ states in the ground state rotational band (GSRB) are coupled with deformation up to β_6 . The results are given in Figs. 5–7.

The Woods-Saxon potential parameters for the coupled channels calculations, given in the low energy notation (V , W , V_{so} , W_{so} , r , a , r_w , a_w , r_{so} , a_{so} , and r_c) are (-3.5 , $+51.9$, 0.66 , and 1.8 MeV, and 1.01 , 0.60 , 1.01 , 0.60 , 1.01 , 0.57 , and 1.05 fm). The deformation parameters are $\beta_2 = +0.47$, $\beta_4 = +0.25$, and $\beta_6 = +0.03$ (solid lines), 0.0 (dashed lines), and -0.03 (dotted lines). The DWBA calculations use the following parameters: (-1.0 , 59.3 , 0.78 , and 2.0 MeV, and 0.95 , 0.69 , 0.95 , 0.66 , and 1.05 fm), with $|\beta_2| = 0.65$ for the 2^+ , $|\beta_4| = 0.38$ for the 4^+ , and $|\beta_6| = 0.14$ for the 6^+ .

Since the 6^+ state is unresolved from a nearby 1^- state, it is difficult to make a quantitative evaluation of the β_6 deformation. The angular distribution for excitation of the 1^- state should be very forward peaked and should fall off faster than that for the 6^+ state. The measured (5.8 , 1^-) angular distribution is scaled to the forward angle data for the 8.7 MeV peak and subtracted to leave what is hoped to be the 6^+ data. The minimum at 19° is deepened somewhat, but the points from 9° to 14° are essentially unchanged. The net result, shown as open circles in Fig. 7, looks much like an $l=3$ or 4 admixture

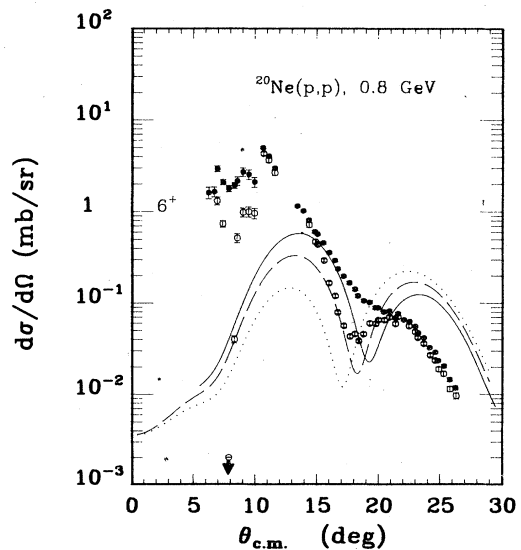


FIG. 7. Angular distribution of protons exciting a group of states including the 6^+ in ^{20}Ne is shown. The open circles are the net result of subtracting the scaled cross sections for exciting the (5.8 , 1^-) state from the unresolved peak. The curves are the same as in Fig. 5.

remains. Thus only a qualitative estimate of the 6^+ cross section can be derived. Varying β_6 between ± 0.03 has no observable effect on the predictions for the 0^+ , 2^+ , and 4^+ angular distributions and analyzing powers. A value of $\beta_6 = +0.03$ has been used here as a reasonable upper limit, but is not determined in this experiment. This value is used in the coupled channels (CC) results for $A_y(\theta)$ given as the solid lines in Figs. 5 and 6 and is assumed in the discussion that follows.

The observed cross section data for the 0^+ , 2^+ , and 4^+ states are reproduced quite well with the coupled channels calculations (Figs. 4–6). The DWBA results are equally good for the 0^+ cross section and analyzing power data, but are a significantly poorer representation of the cross section data for the 2^+ and 4^+ states. Both calculations fail to explain the 4^+ analyzing power data past the region of the first maximum. The coupled channels results do a better job in explaining the 2^+ analyzing power data. Both the relatively large cross section for the 4^+ state and the position of the first minimum in the angular distribution for the 2^+ state are evidence of a large hexadecapole deformation for the ^{20}Ne ground state.

Multipole moments of the deformed optical potentials can be related to those of the matter distributions by Satchler's theorem.⁷ This has been done previously for ^{12}C , ^{24}Mg , and ^{26}Mg .^{2,6} The moments that result from the coupled channels calculations are $M(E2) = 0.164 e b$, $M(E4) = 0.0253 e b^2$, and $M(E6) = 0.0037 e b^3$. $M(E2) = 0.163 e b$ for only 0^+ and 2^+ coupling, $\beta_2 = 0.57$, and $\beta_4 = \beta_6 = 0$ (fit not shown). The magnitude of the 2^+ cross section determines the $M(E2)$ moment, and uncertainty in the strength of the 6^+ has little effect on the determined moments. The 0^+ and 2^+ coupling using only β_2 deformations (not shown) predicts an angular distribution that misses the first minimum in the 2^+ state by about 1° , while the full coupling with a large hexadecapole deformation predicts an angular distribution that is in phase with the data. The DWBA calculations are not in phase with the 2^+ , 4^+ , and unresolved 6^+ data. The remaining differences between the full coupling prediction and the data can be attributed to the restrictive shape for the potential and to the use of the same β_2 coupling between the 0^+ and 2^+ , the 2^+ and 4^+ , and the 4^+ and 6^+ .

There is evidence that the coupling changes as one goes up the rotational band in light deformed nuclei.¹⁹

It is difficult to assign an error to the moments determined from these macroscopic analyses. Optical model uncertainties of ± 0.01 fm in r_w and a_w , ± 0.02 in β_2 and β_4 , and ± 0.03 in β_6 result in uncertainties in the $M(E2)$, $M(E4)$, and $M(E6)$ of $\pm 5\%$, 10% , and 27% , respectively. However, it appears certain that $M(E2)$ and $M(E4)$ are positive and that the $M(E4)$ for ^{20}Ne ($0.025 e b^2$) is large as compared to the values of $+0.007$ and $-0.003 e b^2$ obtained for ^{24}Mg and ^{26}Mg ,⁶ respectively. The $M(E2)$ moment determined here ($0.164 e b$) is slightly smaller than the $B(E2)$ value of $0.171 \pm 0.011 e b$ resulting from the average of electromagnetic studies.²⁰ Some of these measurements are as high as 0.179 – 0.183 .^{21,22} The value determined here is also slightly larger than the $0.150 e b$ value from shell model results using effective charges,²⁰ and $0.159 e b$ from Hartree-Fock calculations.²³

IV. CONCLUSION

Differential cross sections and analyzing powers of 0.8 GeV polarized protons exciting the ground state rotational band in ^{20}Ne have been reported. Coupled channels calculations provide fairly good fits to the observed angular distributions and analyzing powers for the 0^+ , 2^+ , and 4^+ states, and are of reasonable magnitude for the unresolved 6^+ . The results of this study have confirmed the large hexadecapole deformation of ^{20}Ne . The signs of the $M(E2)$ and $M(E4)$ moments of the deformed optical potentials are found to be positive. The value of $M(E4)$ for ^{20}Ne is large compared to other s - d shell nuclei such as ^{24}Mg and ^{26}Mg . Analysis of the data for the excited bands in ^{20}Ne is in progress.

ACKNOWLEDGMENTS

The authors would like to thank the LAMPF staff for their assistance in performing these measurements, and especially Bob Damjonovich for his assistance in the construction of the gas target. The research reported here was supported in part by the U.S. National Science Foundation, the U.S. Department of Energy, and the Robert A. Welch Foundation.

*Present address: University of Maryland, College Park, MD 20742.

†Present address: Los Alamos National Laboratory, Los Alamos, NM 87545.

¹L. Ray, G. S. Blanpied, W. R. Coker, R. P. Liljestr and, and G. W. Hoffmann, *Phys. Rev. Lett.* **40**, 1547 (1978).

²G. S. Blanpied *et al.*, *Phys. Rev. C* **23**, 2599 (1981).

³G. S. Blanpied *et al.*, *Phys. Rev. C* **20**, 1490 (1979).

⁴L. Ray, G. S. Blanpied, and W. R. Coker, *Phys. Rev. C* **20**, 1236 (1979).

⁵M. L. Barlett *et al.*, *Phys. Rev. C* **22**, 1168 (1980).

⁶G. S. Blanpied *et al.*, *Phys. Rev. C* **25**, 422 (1982).

⁷G. R. Satchler, *J. Math. Phys.* **13**, 1118 (1972).

⁸R. de Swiniarski *et al.*, *Phys. Rev. Lett.* **23**, 317 (1969).

⁹R. de Swiniarski *et al.*, *Phys. Rev. Lett.* **28**, 1139 (1972).

¹⁰R. de Swiniarski *et al.*, *Phys. Lett.* **43B**, 27 (1973).

¹¹R. de Swiniarski *et al.*, *J. Phys. (Paris)* **35**, L-25 (1974).

¹²R. S. Mackintosh and R. de Swiniarski, *Phys. Lett.* **57B**, 139 (1975).

¹³H. Rebel *et al.*, *Nucl. Phys. A* **182**, 145 (1972).

¹⁴H. Rebel and G. W. Schweimer, *Z. Phys.* **262**, 59 (1973).

¹⁵R. S. Mackintosh, *Z. Phys. A* **276**, 25 (1976).

¹⁶G. S. Blanpied, M. L. Barlett, G. W. Hoffmann, and J. A. McGill, *Phys. Rev. C* **25**, 2550 (1982).

¹⁷G. W. Hoffmann *et al.*, *Phys. Rev. C* **21**, 1488 (1980).

¹⁸J. Raynal, International Atomic Energy Agency Report IAEA-SWR-918, 1972, p. 281.

¹⁹A. Bohr and B. R. Mottelson, *Nuclear Structure* (Benjamin,

Reading, Mass., 1975), Vol. II, p. 98.

²⁰B. H. Wildenthal, in *Elementary Modes of Excitation in Nuclei*, edited by A. Bohr and R. A. Broglia (North-Holland, Amsterdam, 1977), p. 383.

²¹D. Schwalm, E. K. Warburton, and J. W. O'neal, Nucl. Phys.

A293, 425 (1977).

²²Y. Horikawa, Y. Torizuka, A. Nakada, S. Mitsunobu, Y. Kojima, and M. Kimura, Phys. Lett. **36B**, 9 (1971).

²³Y. Abgrall, B. Morand, and E. Caurier, Nucl. Phys. **A192**, 372 (1972).